Available online at www.CivileJournal.org

Civil Engineering Journal

(E-ISSN: 2476-3055; ISSN: 2676-6957)

Vol. 10, No. 05, May, 2024

Investigating the Hydraulic Behaviours of an Alluvial Meandering River Reach Between Two Barrages

Zainab D. Abbass [1]*, Jaafar S. Maatooq [1], Mustafa M. Al-Mukhtar [1]

[1] *Department of Civil Engineering, University of Technology-Iraq, Baghdad, Iraq.*

Received 29 January 2024; Revised 19 April 2024; Accepted 24 April 2024; Published 01 May 2024

Abstract

The Abassia-Shammia is a meandering stream in Najaf province. Predicting and estimating the flow behavior of meandering rivers is crucial for designing hydraulic structures in an accurate manner in the vicinity and conducting environmental and ecological studies. The hydraulic properties of an alluvial stream are typically subject to change due to its location between two barrages. In this study, HEC RAS 2D, developed by the Hydrologic Engineering Center's River Analysis System, was employed to simulate the hydraulic performance of the Euphrates River reach between two series of barrages, i.e., Abbassia and Shammia. Reliable input data, such as Digital Elevation Models (DEMs), land cover classification, and data for the 2023 hydrograph as a boundary condition, were utilized to develop the hydraulic model. The model was calibrated by using the observed water surface elevation from field measurements downstream of Abbassia to match the ones calculated by the model. Hence, the hydraulic model of the Euphrates River was created using an appropriate Manning roughness coefficient value (n = 0.04) based on the most suitable values of statistical indices, correlation coefficient (R^2), and root mean squared error (RMSE) to assess the agreement between the observed and simulated data throughout the calibration and validation phases. To visualize the HECRAS2D output, the hydraulic maps for the study region were presented. The ten cross-sections from the field study (investigated at the same period of flow hydrograph) were presented for modeling to emphasize the river's hydraulic behaviors. Based on the results, the water surface elevation ranged between 19.1–29.2 m.a.s.l., and the flow velocity was 2.50 m/s. Meanwhile, the values of bed shear stress (Pa) and the water depth (m) ranged between 0.1 Pa and 8.93 m for the entire river. The results also proved the superiority of the HEC RAS2D model to reliably represent the hydraulic performance of the Euphrates River reach located between the two barrages.

Keywords: Hydraulic Behavior; Abbassia-Shammia Barrages; Euphrates River; Alluvial Stream; HEC RAS 2D.

1. Introduction

The flow behavior in natural channels, such as rivers, is a complex phenomenon due to the complex hydraulic properties of the unstable and non-uniform flow [1, 2]. To complete water resource management, various hydraulic structures must be constructed. These structures alter the hydrodynamic and geometric behavior of the affected reaches due to the presence of upstream and downstream. For example, the construction of a barrage to do its functions leads to a decrease in the flow velocity along the backwater profile upstream, which causes the deposition of suspended sediment in some regions and erosion in others. On the other hand, a reverse action will dominate downstream by increasing the chances of banks and bed erosion. The study of flow patterns around bends and meandering sections of rivers is of great importance to engineers since it is an essential field of research to determine the hydraulic flow in these regions [3].

* Corresponding author: bce.19.83@grad.uotechnology.edu.iq

http://dx.doi.org/10.28991/CEJ-2024-010-05-013

Previous studies, for example, Whiting & Dietrich (1993) [4], Whiting & Dietrich (1993) [5], and Blanckaert (2009) [6], have explored this topic analytically. However, contemporary approaches, such as numerical modeling, used by many researchers such as Ulke et al. (2017) [7], Hsieh and Yang (2003) [8], and Darby et al. (2002) [9], are now being used to study the flow in river bends and meander stretches. In this study, the authors employed the HEC-RAS River Analysis System 2D Modeling to perform the necessary numerical simulations. Brunner (2016) [10] provides a comprehensive and thorough concept presentation. A numerical model is faster to set up and to simulate for the same changes.

Many studies on the hydrodynamic action of rivers were carried out based on field investigations and numerical models. Elbashir (2019) [11] performed a study including a 2D quasi-unsteady state model at five discharges on a 23.5 km reach of the lower Wairau River to quantify its hydraulic geometry. A high-resolution multispectral aerial image was used for in-depth mapping. The findings showed that, as for comparing within the study area, the upper reach reacts to increasing river flow with higher changes in width, the lower reach with higher changes in depth, and the middle reach with slightly higher changes in velocity. Kayyun & Dagher (2018) [12] presented a study for a reach with a length of 19.5 km lying in the northern part of the Tigris River between Al-Muthanna Bridge and Sarai gauging station at Baghdad city in Iraq and used a model for 2D unsteady flow for calculating the velocity and water surface elevation for the flooding scenarios of flow rate.

Zahraa et al. (2021) [13] conducted a field data acquisition survey at 38 locations to examine the water flow in the Tigris River. These stations were selected to develop one-dimensional unsteady numerical flow models using HEC-RAS software. The key findings of the steady and unstable state models were the highest rate of flow, velocity, and smallest cross-sectional area of flow at designated locations. The findings of their research can assist in identifying the sites where flow is restricted, leading to faults. Additionally, their findings can serve as a foundation for establishing the crucial locations where sedimentation occurs and causes changes in the bed level along the Tigris River. Vedmani et al. (2020) [14] performed a study using HEC-RAS for the hydraulic analysis of the Nagpur minor canal irrigation system. Hydraulic models are the basic tools for understanding the hydraulic flow behaviors of open channels. Manning's roughness is a very sensitive parameter in the development of hydraulic models, where it is necessary to calibrate the values of this coefficient based on the features of a river boundary.

Donald (2017) [15] used HECRAS2D to compare 1D and 2D models for the floodplain's inundation and the channel water level. Two approaches for solving the issue were investigated: Floodplain units were discretized into storage regions to create a 1D model; a channel and the floodplain surface were modeled in 2D. Bear Creek and the Great Miami River served as study areas for the two models. The models were evaluated by contrasting them with the extent of the measured flooding. The author also examined the mathematical basis for predicting floodplain flow using a two-dimensional approach. Ghimire (2019) [16] computed and compared the predictive capabilities of 1D, 2D, and linked 1D/2D HEC-RAS models to determine the extent of the flooded area and the duration of flood travel, which are necessary for a flood warning system. The Grand River in Ohio's Lake County served as the study site. The study aimed to demonstrate the HEC-RAS 2D model's capacity to replicate the evolution of a braided river.

Balouchi et al. (2022) [17] assessed the Braided Index (BI) variation in the chosen reach over the input time of the hydrograph. The researcher provided an applied context in which future modeling challenges can be taken into account. The Devoll River in Albania was simulated using a two-dimensional (2D) depth-averaged approach, HEC-RAS. Parhi et al. (2012) [18] attempted to employ HEC-RAS software for simulating floods to calibrate the channel roughness coefficient, also known as Manning's "n" value, along the Mahanadi River in Odisha. A simulation was carried out for the flood that occurred in the same river reach in 2006, using a calibrated model that took into account the channel roughness. The performance of the HEC-RAS-based model, which was calibrated and validated, was evaluated using the Nash and Sutcliffe efficiencies. Based on the simulation study, it was determined that the Mahanadi River section from Khairmal to Munduli produces the most favorable outcomes when Manning's "n" value is set to 0.032.

Anderson (2022) [19] performed a study contrasting a baseline's hydrologic condition year (2010) to Kozak et al.'s (2016) [20] environmental flow prescription. The outcomes of the flooding have a bearing on cypress regeneration and hydraulic connectivity. Several data sources were used to build the hydraulic model, which was then refined via vertical feature (VF) extraction and then calibrated and validated. The digital elevation model (DEM) was produced by combining information from several topographic and bathymetric sources. Above all, this incorporated the back-swamp bathymetry. They supplied polylines of important VFs in the DEM, like natural levees. The VFs and cell faces of the HEC-RAS mesh, which is used to compute flow, were lined up. The model was calibrated for both high and low flow periods to accurately represent the hydrodynamics throughout the year. The 2010 hydrograph served as the model's validation dataset.

Khuzaiea et al. (2018) [21] constructed the results of a hydraulic model used to measure the surface friction roughness (Manning's coefficient) of the Euphrates River along a 110-kilometer stretch in the Al Muthanna Governorate of Iraq. Hydraulic modeling was the method used for determining the surface friction coefficient. The HEC-RAS hydraulic model was initially fed with surface friction roughness values, which typically vary from 0.025 to 0.04 for open natural channels. When the computed surface roughness value in this study was compared to the observed values, it was discovered that a value of 0.04 produced the best agreement with the model.

Hameed and Ali (2013) [22] evaluated (n) in the Al-Hilla River in Iraq using the HEC-RAS flow model. For the whole river, the best agreement value between the computed and observed hydrographs was (0.027). Hameed (2014) [23] found (n) in the Al-Kufa River in Iraq and predicted a value of roughness of (0.032) by creating the HEC-RAS flow model calibration, which also indicates the best agreement between the computed and observed hydrographs.

Serrano et al. (2024) [24] investigated the hydraulic aspects of flood formation in the Marikina River floodplain during Typhoon Vamco, utilizing HEC-RAS numerical modeling. The outcomes of the model can be utilized to implement strategies aimed at reducing both the likelihood and severity of potential risks and damages. Orozco et al. (2023) [25] evaluated the performance of both HECRAS2D and TELEMAC-2D software by comparing the flood results and describing their performance, capabilities, limitations, and the study of levee breach scenarios. Garg and Ananda Babu (2023) [26] employed a high-resolution 2D HEC-RAS model to accurately simulate the flood events that took place in 1994, 1998, 2002, 2006, and 2015. This was demonstrated to illustrate the importance of channel roughness as a crucial element in developing a hydraulic model for predicting floods and mapping the area affected by floodwaters. The results demonstrate a robust link between the simulated and observed floods. Mawat & Hamdan (2023) [27] utilized the HEC-RAS2D software to conduct a 2D hydrodynamic model for the Shatt Al-Arab River. Mohamed et al. (2023) [28] assessed the flood wave characteristics that arise from a dam breach caused by a piping failure within the dam structure and the subsequent transmission of the flood waves using HEC-RA2D software.

The Abbassia-Shammia Reach is the main section of the Euphrates River, providing water for communities located on its banks. The Euphrates River is widely recognized as one of the most important ancient rivers on a global scale. The river is remarkable for its status as the longest in southwest Asia, measuring 2786 km in length and having a drainage basin of around 440,000 km^2 [29].

There remain several aspects of hydraulic behavior that have not been thoroughly studied. The Abbassia reach, spanning 32 kilometers from Abbassia city in Kufa to Al-Shamiya city in Dywania, has not been previously examined for changes in water flow. In 1982, the Iraqi Ministry of Water Resources (IMoWR) initiated the construction of the Abbassia and Shammia barrages. The barrages are located downstream of the Babylonian governorate. The existence of potential alterations in the flow within this specific region emphasizes the necessity for a comprehensive examination of the hydraulic properties. The majority of writing on Abbassia-Shammia mostly focuses on the geometric characteristics and/or composition of the bed material. The main methodology utilized in this research consists of a cross-sectional survey as well as laboratory investigations of bed materials and field surveys. These methods were adopted for analytical comparison with global equations.

The sources cited are Kareem Abed et al. (2014) [30], Hobi (2014) [31], and Mahmood et al. (2017) [32]. These studies only prioritize fieldwork and laboratory work, disregarding research on the hydraulic behavior of the rivers.

This study is a pioneering attempt to understand reach behavior using on-site data, including the available data that was officially requested from IMoWR. The analysis was conducted using HECRAS2D software. Previous research has mainly focused on one-dimensional aspects of the river, ignoring the transverse or vertical directions of the river.

The HECRAS2D model was used for calibration and validation of the sets of observed water depths before simulating a water depth. The model was run with different values of (n) ranging between 0.02 and 0.04, and the calibrated value obtained was 0.04 for ten locations. Model performance has been tested using the R^2 and RMSE statistical criteria. There has been relatively superior calibration and validation for the model at the ten locations.

This study aims to assess the hydraulic behavior downstream of Abbassia Barrage by applying hydraulic modeling tools HEC-RAS2D with the RAS Mapper tool to investigate the river state. Also, using the digital elevation model in the RAS mapper allows users to develop geometric data for easy use of HEC-RAS and view all river hydraulic result data. To that point, a field measurement was conducted at the Euphrates River between the Abbassia and Shammia barrages to view the effect of flow on the river behavior.

2. Study Area

The Abbassia-Shammia Barrage was selected as a study area. The Abbassia Barrage was constructed on the Kifil-Shanafiyah branch of the Euphrates River downstream in Babylon governorate for irrigation purposes in 1982. The barrage function is to regulate and manage the flow in the middle of the Euphrates region. The design discharge of the barrage is 1000 m^3/s, with a downstream water level of 23.8 m. In recent days, the operational discharge ranges from 30 to 60 m^3/s with a water level, as mentioned in the operational report, of 23.5 m. Each barrage contains six rectangular openings, each with a dimension of 12 m in width and 6 m in height, equipped with a steel radial gate. The length of the study reach is 32 km between the Abbassia and Shammia barrages. Figure 1 shows the location of the Abbassia-Shammia Barrage and the course of the river covered by the study.

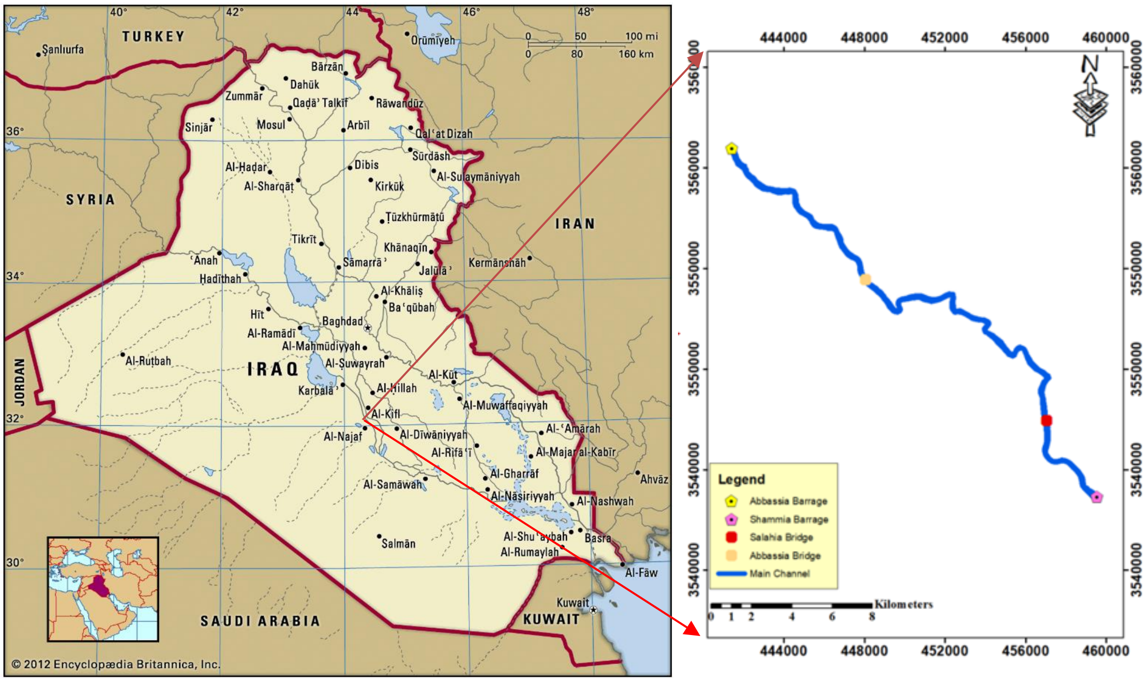

Figure 1. Illustration of the study area

3. Material and Methods

3.1. Data Collection and Processing

This study presents the results of the hydraulic model, utilizing a flow hydrograph for the year 2023 obtained from Ministry of Water Resources [33] for the Abbassia-Shammia River as a boundary condition in HECRAS2D. The study will be conducted for one year. The objective of this section is to simulate the hydraulic characteristics of the study area. A bathymetric survey was conducted using the Acoustic Doppler Current Profiler (ADCP) to measure both water depth and discharge. An essential requirement for creating a hydraulic model is a series of cross-sections (CS) that span the whole channel. Historically, these models have been developed by conducting inspections of numerous cross-sections of the stream segment that is to be replicated. The authors collected the data for river cross-sections (CS) by field inquiry. Regarding the Abbassia-Shammia Stretch, there have been two recent sets of cross-sections collected. One set consisted of four cross-sections taken up until March 22, 2023. The second set functioned as six control systems until May 17, 2023, and both sets were utilized during the simulation time. The findings indicate that the mean slope energy was 0.0001, with a progressive decline in slope from Abbassia Barrage to Shammia Barrage at a distance of 32 km. The recorded flow velocities ranged from 0.011 to 0.174 m/s, with the highest velocity seen at (CS7) located downstream of Abbassia Barrage, at a distance of 20 km. The positions of the ten cross-sections are indicated in Figure 2 below. Figure 3 displays several images captured during the field research.

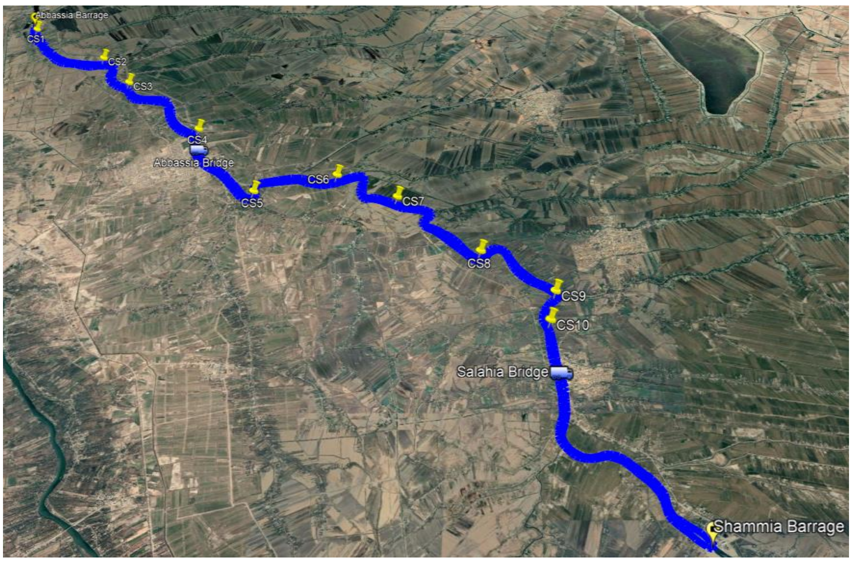

Figure 2. The cross-section's locations where the model is calibrated and validated

Figure 3. Field investigation through the study area

3.2. Methodology

The HEC-RAS 2D 6.3.1 model of the digital elevation model (DEM) data was used in this study. The initial stage of this project involves gathering data through a field survey using the Acoustic Doppler Current Profiler (ADCP) to obtain essential measures for rivers, including water depth, velocity, and flow discharge. These measurements are crucial for the calibration and validation procedures. A total of ten cross-sections were generated spanning the whole length of the river. The flow hydrograph from 2023 was utilized as a boundary condition in the input data for HECRAS2D for one year. This was conducted to examine the hydraulic performance of the river and analyze its behavior using measurements taken at ten cross-sections. The RAS mapper and DEM geometry files were generated, and Manning roughness was calibrated using sections obtained from the field survey. Once the 2D region was established in the RAS mapper, a mesh was formed, a hydraulic file was prepared, and the model was developed following the flow chart. Figure 4 displays the schematic illustrating this process.

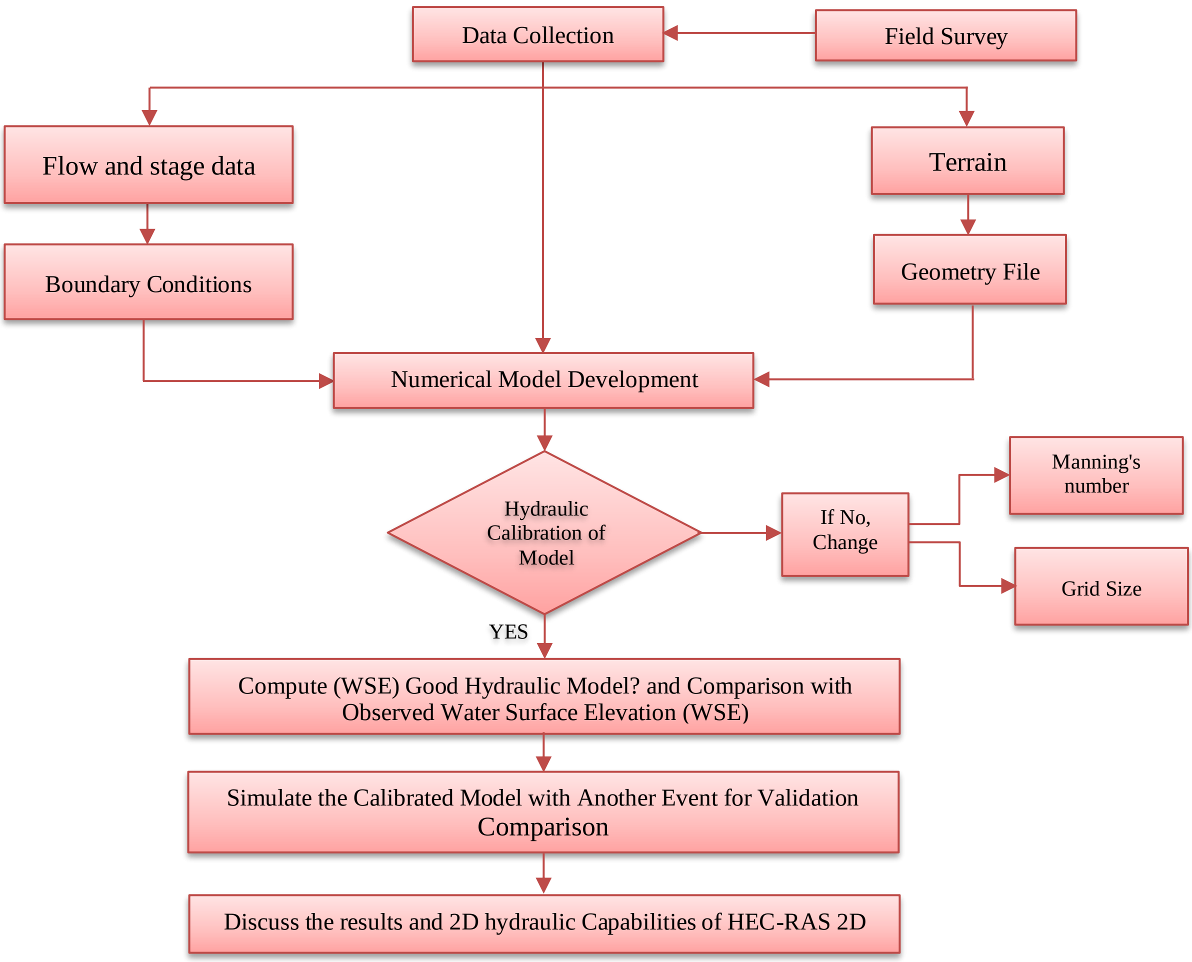

Figure 4. Methodology flow chart for the study area

3.3. Numerical Model Development

The numerical model is constructed using a hydrograph of flow and stage from the 2023 data from the Abbassia reach of the Euphrates River, which spans for one year. The hydrograph of water flow measured at the Abbassia-Shammia reach, located 32 km downstream of the Abbassia Barrage, provides information about the volume of water entering this section of the Euphrates River. In 2023, when the data were collected, the highest average monthly flow into the Abbassia-Shammia reach was 44.26 m^3/s, with the peak occurring in December. In June 2023, the upstream of Shammia Barrage, which is located downstream of the Abbassia Barrage, experienced the lowest discharge of 19.68 m^3/s. In June 2023, the data indicate that the highest average monthly stage of 19.2m was observed. However, in February 2023, the International Monitoring of Water Resources Institute (IMoWRI, 2023) recorded the lowest level of 18.67 meters, as depicted in Figures 5 and 6. Diverse results were utilized to create the model. This document provides a concise overview of the input data and the sequential actions involved.

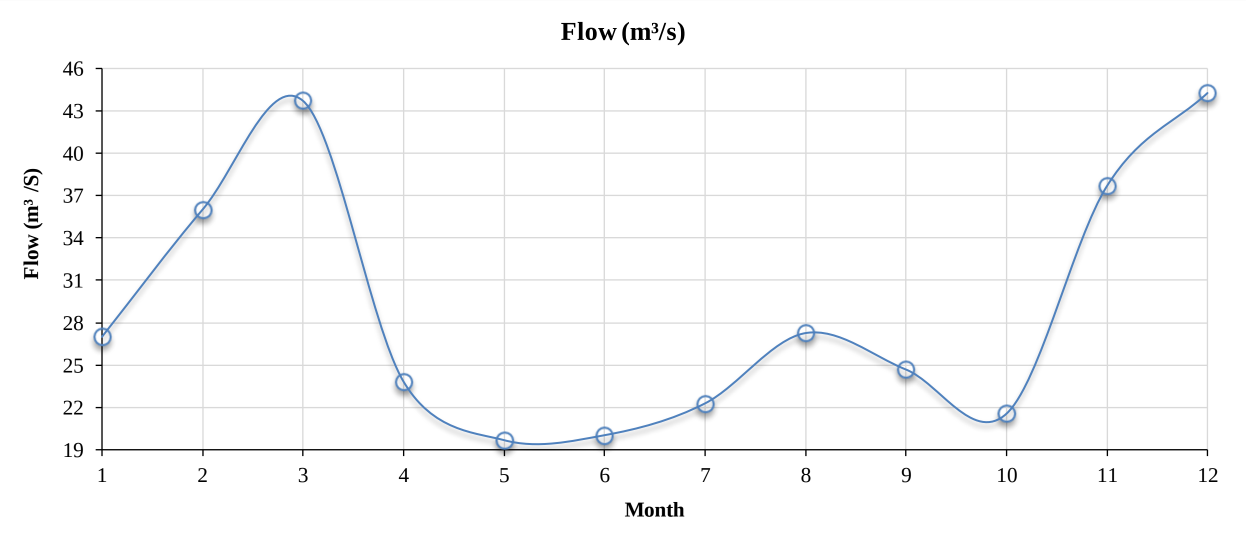

Figure 5. Flow hydrograph recorded upstream of Abbassia-Shammia reach in 2023

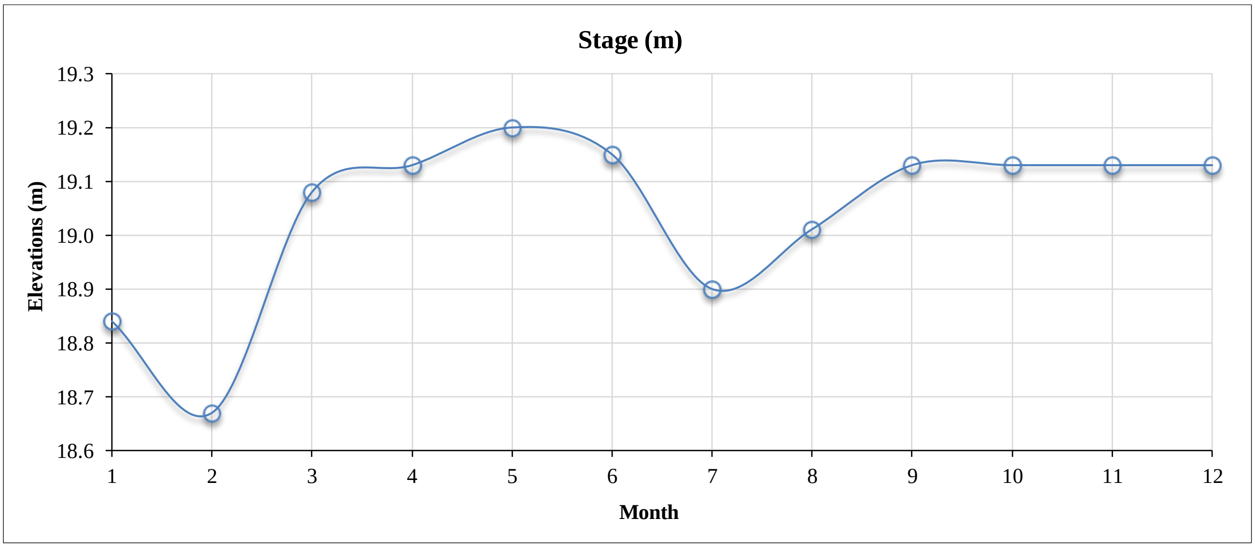

Figure 6. Stage hydrograph recorded at downstream of Abbassia-Shammia reach in 2023

3.3.1. Terrain Model

To achieve a precise hydraulics model, it is necessary to have a comprehensive terrain model. Digital Elevation Models (DEMs) are essential elements in any modeling or numerical analysis that pertains to the topography and elevations of the Earth. The digital elevation model (DEM) for the research area was obtained from the USGS [34] website and utilized to generate the terrain file for the numerical model. HEC-RAS utilizes a gridded model to represent the landscape. Therefore, a high-quality terrain model was generated with a grid dimension of 20×20 m. The terrain utilized in this study is depicted in Figure 7 and is employed in HEC-RAS 2D.

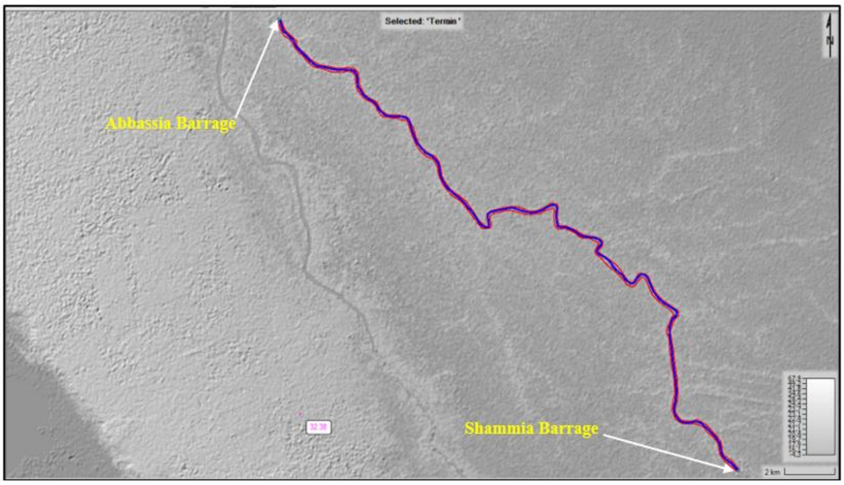

Figure 7. Digital elevation model for study area

3.3.2. Development of Structured Grid

Efficient grid creation is a vital task in numerical modeling. The correctness of results in 2D flow regions is largely dependent on the careful selection of appropriate mesh cell sizes and computational time steps (ΔT). In the initial phase, a computational mesh is generated with cell dimensions that are appropriate for simulating the topography and hydrodynamics of water runoff. To establish a proficient computational mesh in HEC-RAS2D, it is imperative to verify that the cell faces precisely depict the utmost point of flow obstacles. Optimal cell dimensions must be employed at the designated site to precisely depict the fluctuating water surface and velocity [35]. Therefore, the model is assessed using the smallest mesh size (20×20) comprising 7318 cells, as depicted in Figure 8, to ascertain the most favorable outcomes. By using these cell sizes, the stability of the model was confirmed, and it functioned flawlessly without any errors. The time step in the HEC-RAS simulation represents the length of each computation period. The selection was based on the grid size and flow velocity. By employing the fixed time step (basic technique) in HECRAS2D, the calculation time interval was approximated to be around 15 seconds.

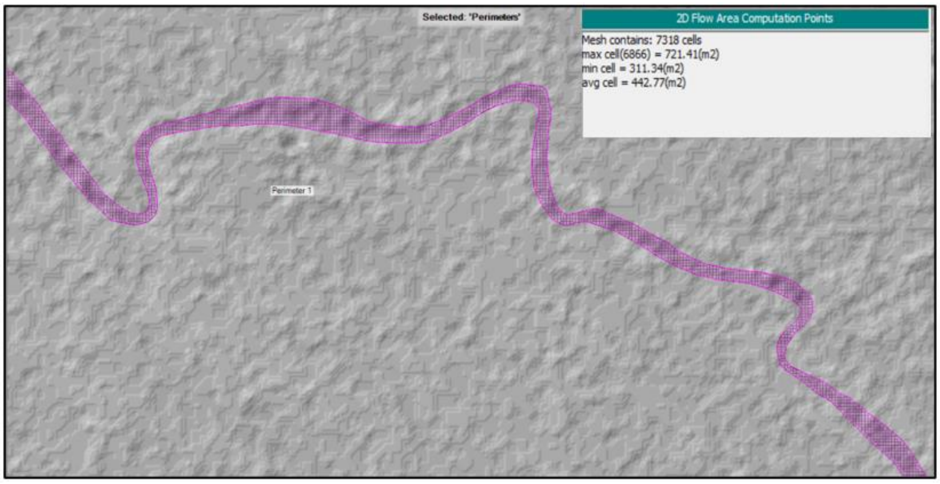

Figure 8. River mesh size (20×20) with 2D Flow area computations characteristics

3.3.3. Boundary Conditions and Set of Equations

The one-year flow hydrograph, spanning from January 1, 2023, to January 1, 2024, was utilized as upstream boundary conditions to represent the hydraulic conditions of the flow area. These conditions align with the calibration period for the observed cross-sections. A stage hydrograph with the same flow duration was employed as the downstream boundary condition, taking into account the fluctuating water surface level. In HEC-RAS, the default setting is to use the diffusion wave equations. However, it is advisable to test the Shallow Water Equations (SWE) if they are required for a specific application. As stated in the HECRAS2D user manual [35], a common method is to employ the diffusion wave equations while constructing the model and addressing all issues, unless it is established that the whole Saint-Venant equations are necessary for the specific dataset being modeled. After ensuring that the model is functioning well, it is possible to create a second HEC-RAS plan to change the equation set to the SWE option. It is worth noting that the SWE option typically necessitates a smaller computation interval compared to the diffusion wave approach to maintain stability throughout execution. The second plan will be executed, and the two responses will be compared throughout the entire system. If there are any notable disparities between the two runs, it is advisable to consider the Saint Venant Equations (SWE) as the more precise option. Therefore, this equation should be utilized for model calibration and other event simulations [35]. The study incorporates the Saint Venant Equations (SWE) into the model without any indication of a mistake. The shallow water equations (SWE) are a system of equations that describe the behavior of a thin layer of fluid in a state of hydrostatic equilibrium. They enable the simplification of three-dimensional analysis while maintaining an adequate level of justification for the real event. The Shallow Water Equations (SWE) postulate that the vertical length scale is significantly less than the horizontal scale. Brunner (2022) states that the assumptions of hydrostatic pressure, uniform density, and incompressible flow are made. If the flow is assumed to be incompressible, the continuity equation can be represented by Equation 1:

$$\frac{\partial h}{\partial t} + \frac{\partial (hu)}{\partial x} + \frac{\partial (hv)}{\partial y} = q \tag{1}$$

where, t is time (T), h is water depth (L), u and v are velocity components in the x and y direction respectively. Q is source/sink flux term.

4. Results and Discussion

4.1. Generation of Land-Cover Data from Satellite Images

The coefficient of roughness (Manning's n value) for 2D flow regions in HEC-RAS 2D modeling is often associated with land cover classes. The roughness coefficient (n) in natural channels is difficult to determine in a field. Various factors affecting the values of roughness coefficients were presented by Chow [36]. In this study land cover classification was downloaded from the Esri website [37], then imported to the RAS Mapper in HECRAS2D at the end, associated with the terrain and geometrical file in the RAS Mapper. Table 1 and Figure 9 display the range of Manning's n values used for each land cover classification and its corresponding value in the National Land Cover Database (NLCD) [35].

Table 1. Roughness coefficient for land covers classification of NLCD

NLCD Value	Land Cover Definition	Range on n Value
11	Open Water	0.025-0.05
21	Developed, Open space	0.03-0.05
22	Developed, low Intensity	0.08-0.12
24	Developed, High Intensity	0.12-0.2
43	Mixed Forest	0.1-0.16
71	Grassland/Herbaceous	0.07-0.16
81	Pasture/Hay	0.025-0.05

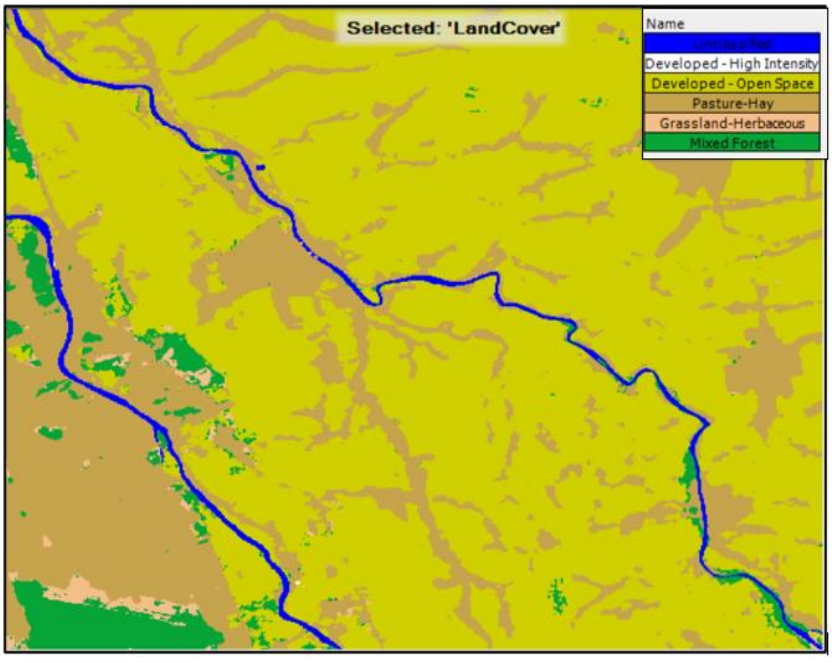

Figure 9. Region classification of the land cover layer

4.2. Calibration and Validation of the Coefficient of Manning Roughness

Calibration is the act of modifying the parameter values of a model to accurately replicate the real-world response, while conforming to certain performance standards that determine an acceptable amount of adjustment between the model and reality [38, 39]. From the literature reviewed previously according to Hameed and Ali (2013) [22], Hameed (2014) [23]; Mustafa et al. (2017) [40], the value of Manning ranged between (0.03 and 0.04). Statistical indicators R2 and RMSE were used for calibration and verification, according to Akay et al. (2016) [41], and Vedmani et al. (2020) [14]. In the present study, the data (10CSs) were used for calibration purposes, i.e., evaluation of Manning's coefficient for the reach under study. This is examining the model with actual data to achieve its predictive precision.

In this paper, the proposed values of the Manning roughness coefficient (n) were taken within the range of 0.030–0.040. The results of the model for the estimated values of water surface elevation at different values of (n) were compared with the observed water surface elevation measured at ten cross-sections (CSs) using root mean square error as a statistical indicator. The results show that implementing the values of (n) in a value of n = 0.04 gives the closest agreement between the observed and computed (WSE) with $R^2 = 0.8871$ and RMSE = 1.19, as shown in Figures 10 and 11.

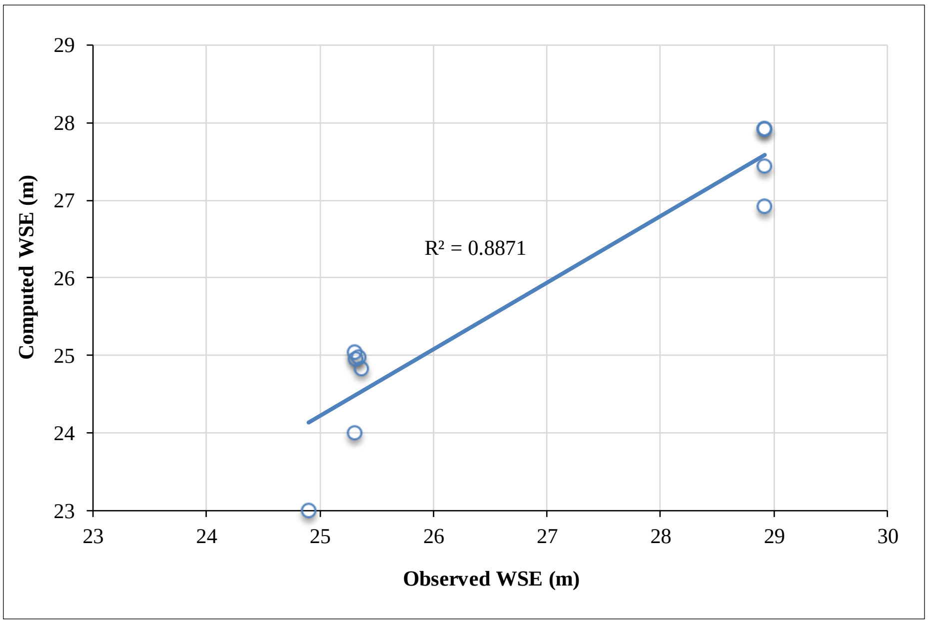

Figure 10. Trendline for calibration Process

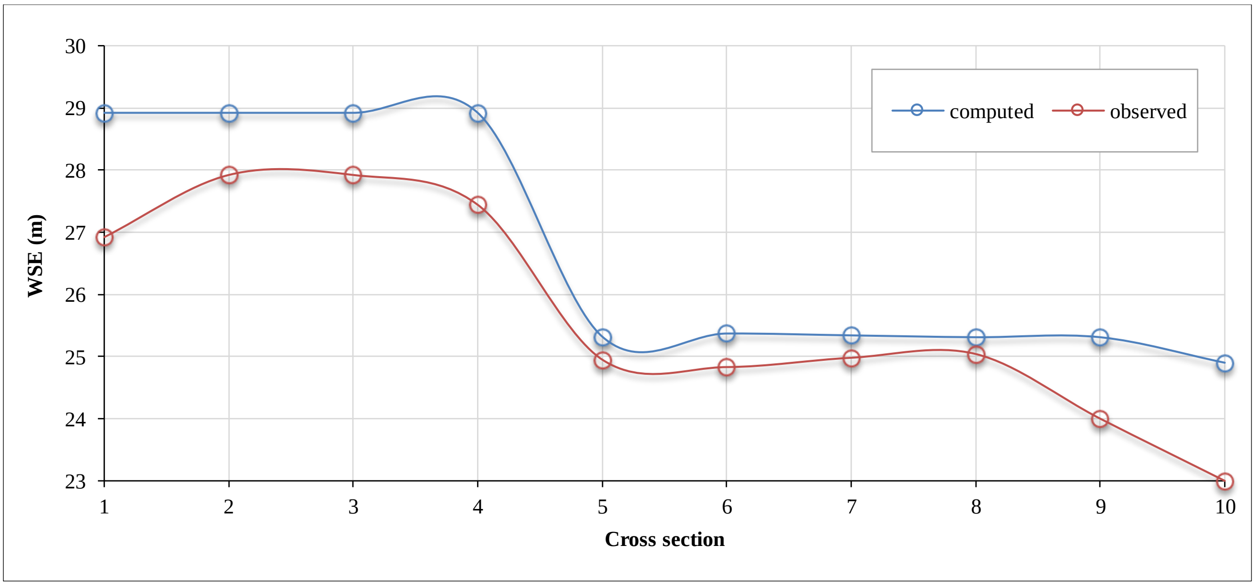

Figure 11. Measured vs. Computed WSE along the river with 10 CSs (for Calibration processes)

The benefit of the validation is to verify the results of the 2D unsteady flow model. Verification is an important task in analyzing the accuracy and uncertainty of the model. The validation of 2D unsteady flow can be performed using the estimated flow velocity from the model compared with flow velocity records for ten measured cross-sections (CSs). Figures 12 and 13 illustrate the comparison that was done for downstream reach at n = 0.04 and R^2 = 0.7972, RMSE = 0.04898.

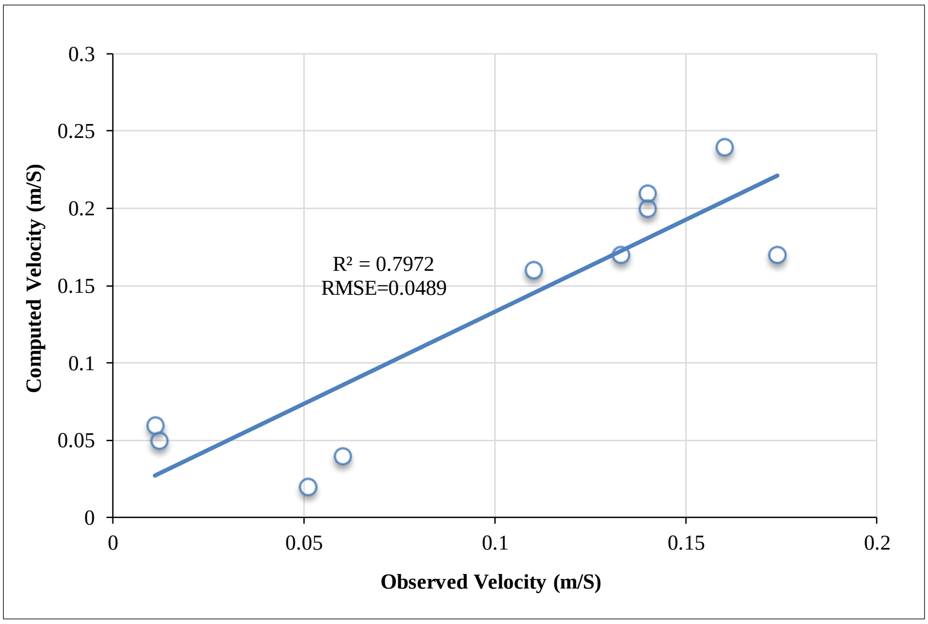

Figure 12. Trendline for Validity Process

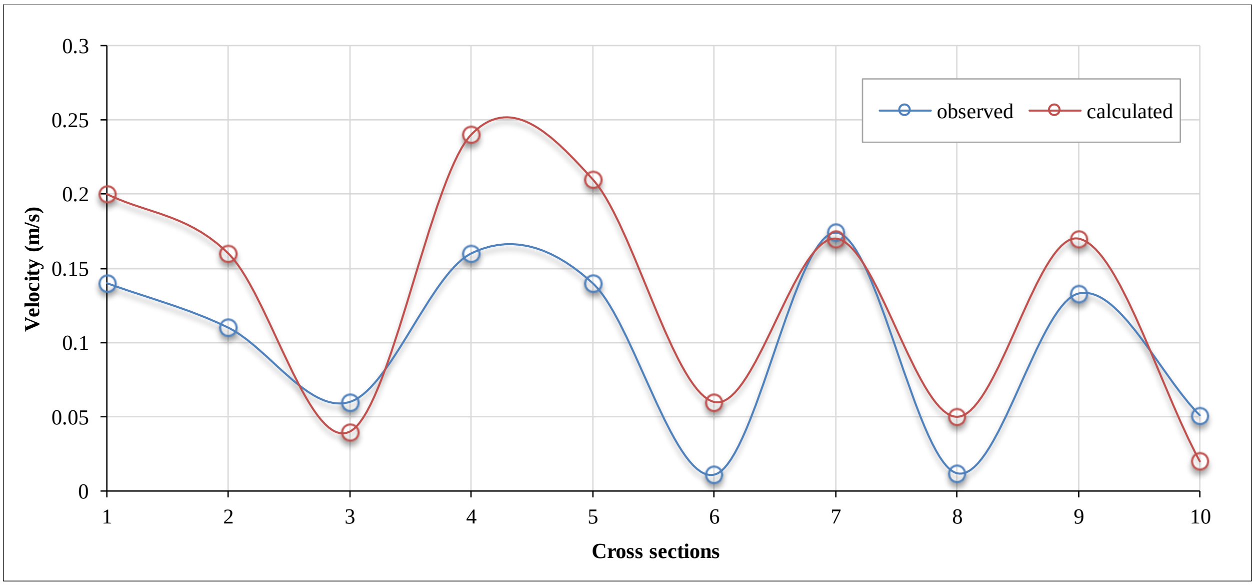

Figure 13. Observed vs. Computed flow velocity with 10CSs for Validation processes

4.3. 2D Unsteady Flow Hydraulic Simulation

The Abbassia-Shammia is a meandering river characterized by a prominent serpentine shape. The hydraulic characteristics maps were generated by plotting the processes using a one-year flow hydrograph from 2023 as the input boundary condition, and a matching stage hydrograph from the same period as the outlet boundary condition for the entire river. Figure 14 shows the velocity results spatially presented for a holistic understanding of the study region for a particular purpose. For velocity, the maximum value was (2.50) m/s, while for other hydraulic characteristics of the river such as depth, water surface elevation (WSE), and shear stress, the maximum values were (8.93) m, (29.2) m, and (0.100) pa, respectively. The variation of the velocity and water depth through straight and meandering sections were visualized through ten measured cross-sections. Figure 15 shows the maximum value appearing at meandering cross-sections, CS7, and CS9 while it appears near a constant rate of variation in straight cross-sections (CS1, CS2, and CS3). Figure 16 shows the depth variation at a high level at straight cross-sections (CS1, CS2, CS3, CS4, and CS10) and a low rate at other meandering cross-sections.

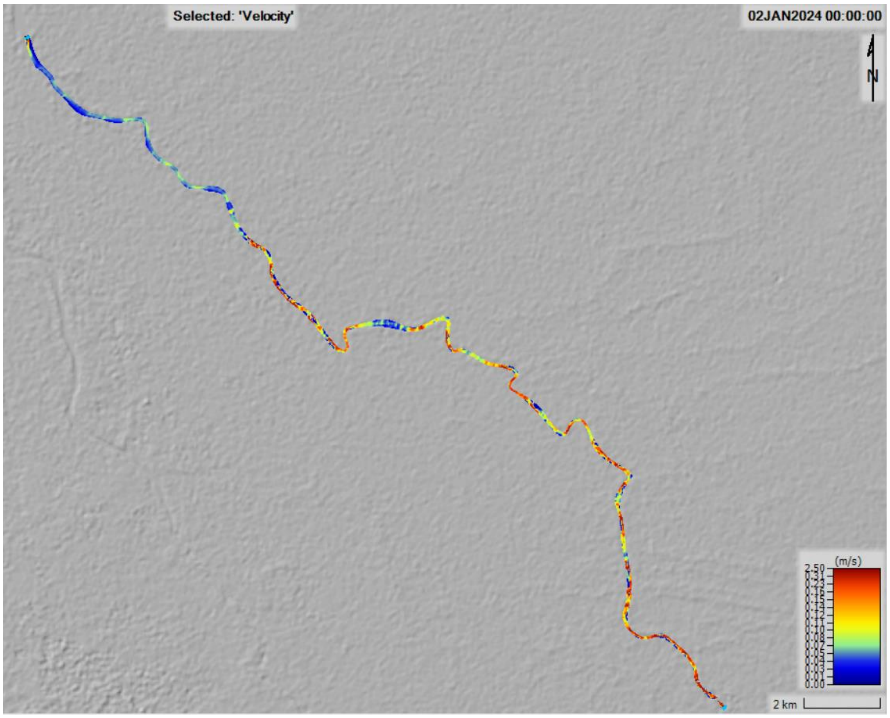

Figure 14. Velocity distribution in the study area

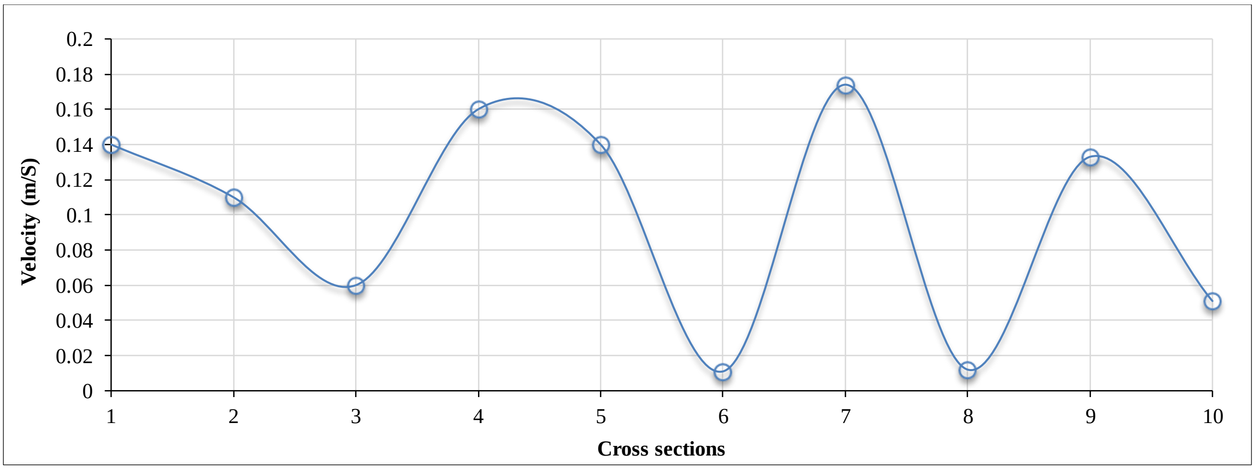

Figure 15. velocity variation through ten cross-section field investigation

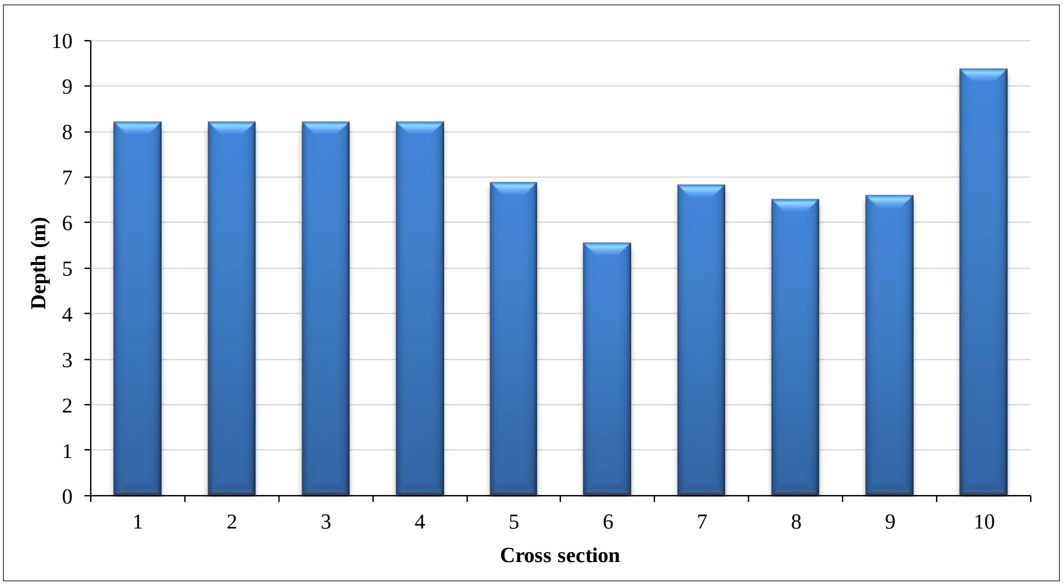

Figure 16. describe depth variation through ten cross-section field investigation

The research region is characterized by regular gradational variations in the cross-sectional area, channel planform, and river shape. An analysis of hydraulic behavior in the river was conducted by examining ten measured cross-sections along the stretch under study. An unexpected increase in velocity (shown by the color red) has been observed at specific spots within the river regions. The sudden rise in water level is attributed to the narrowed cross-section of the river, the disparity in elevation between two spots along the river's path, and the presence of vegetation outside the river's boundaries, as seen in Figure 17. Conversely, there is a noticeable reduction in speed (shown by a yellow or blue hue) along the river at specific locations. This is due to the presence of an island, the wider cross-section of the river, and the existence of vegetation within the river itself, as seen in Figure 17. Figure 18 displays the spatial distribution of shear stress, ranging from greatest (shown by the color red) to minimum (indicated by the colors yellow or green), for simulating shear stress. At the point when the flow transitions from the straight section to the curved section, the highest shear stress occurs along the inner edge of the main channel. Nevertheless, the thread experiencing the greatest shear stress gradually shifts toward the centerline of the channel in the straight section, as depicted in Figure 19.

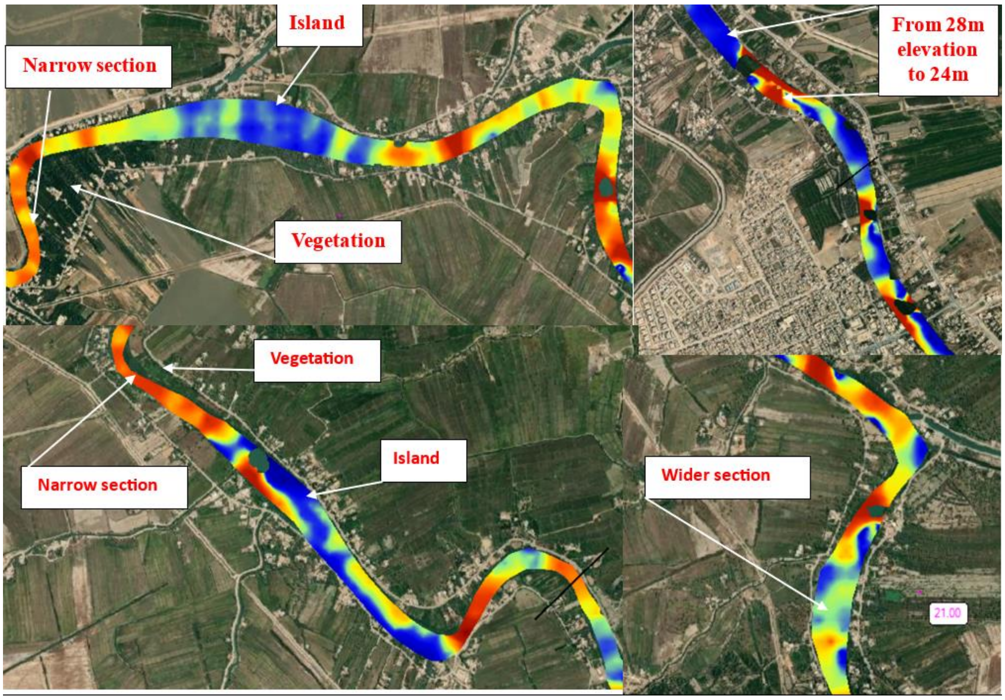

Figure 17. describe different cases of river velocity in the study area

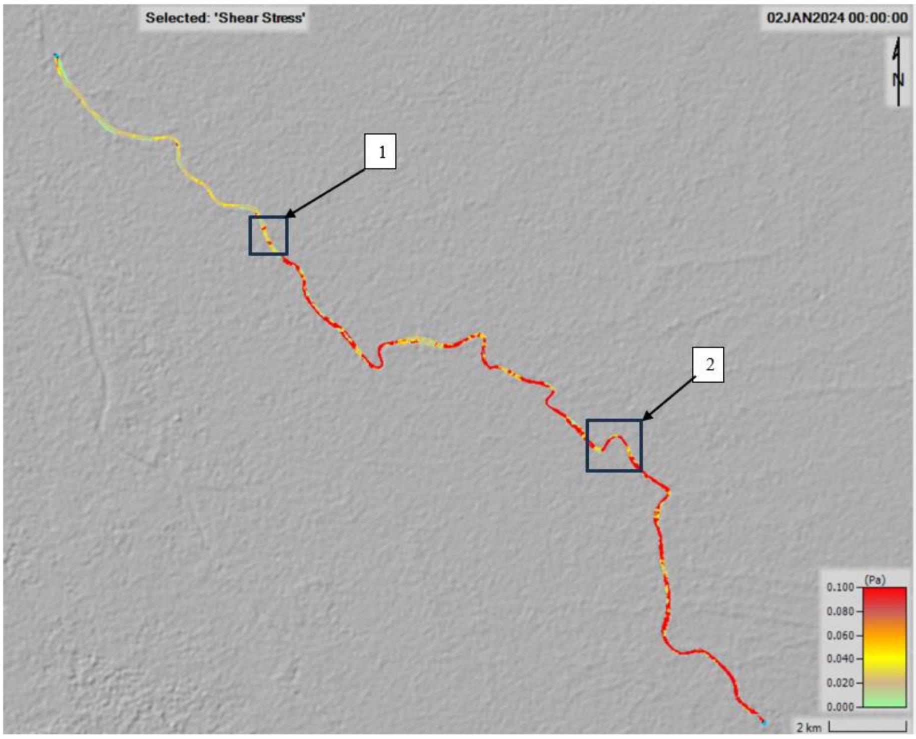

Figure 18. Shear stress distribution in the study area

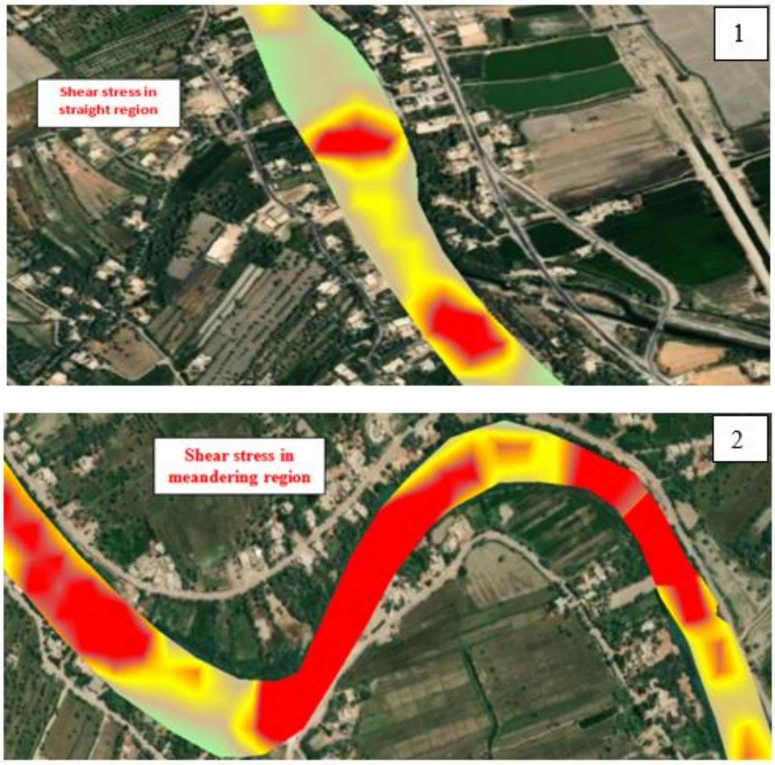

Figure 19. describe shear stress in meandering and straight regions

5. Conclusions

This study utilizes the HEC-RAS 2D 6.3.1 model to analyze data from the digital elevation model (DEM) for the hydrograph of flow and stage throughout 2023. The data collection for this project commenced with a field survey employing an Acoustic Doppler Current Profiler (ADCP) to get the requisite information for rivers, encompassing water depth, velocity, and flow discharge. Ten cross-sections were measured for calibration and validation purposes to determine the Manning roughness. A geometry file was created using the RAS mapper and DEM. After creating the 2D region in the RAS mapper, meshing was generated, and a hydraulic file was created to analyze the influence of flow on the hydraulic efficiency of the river. The hydraulic findings for the entire river at each measured and plotted cross-section put forward the following conclusions:

- The utilization of Abbassia and Shammia Barrages on the Euphrates River illustrates how the interactions between the upstream and downstream barrages combine to create a distinct hydraulic behavior for the river.
- The calibration and validation processes were carried out, and the results reveal that Manning's roughness coefficient (n) has a value of 0.04. This value signifies the best degree of agreement between the measured and computed cross-sections for the specific area under study.
- Within the specific stretch being examined, the river undergoes a significant increase in velocity as a result of its narrower width, the variation in elevation between two spots along the river, and the presence of vegetation surrounding the river at these locations. Conversely, the island's presence, together with its wider cross-section and vegetation within the river, leads to a significant decrease in velocity at specific points throughout the whole river.
- The velocity variation in straight and meandering sections was observed using ten measured cross-sections. The results show that the highest velocity values occur at meandering cross-sections CS 4, CS 7, and CS 9, while the velocity remains relatively constant in the straight cross-sections (CS 1, CS 2, and CS 3).
- The fluctuation of water depth between straight and meandering sections was observed by measuring ten cross-sections. The results show that the depth variation is significant for the straight cross-sections (CS 1, CS 2, and CS 3) and (CS 10) for the meandering cross-sections.
- The maximum shear stress occurs at the inner boundary of the main channel when the river transitions from the straight part to the curved segment, as determined by a shear stress simulation. However, the thread experiencing the greatest shear stress gradually moves towards the centerline of the channel in the straight reach zone.

However, based on the obtained conclusions, it is recommended that a thorough investigation be conducted into the interconnections between the series of barrages, considering other hydraulic aspects such as depth velocity and stream power.

6. Declarations

6.1. Author Contributions

Conceptualization, Z.D.A. and J.S.M.; methodology, Z.D.A. and J.S.M.; software, Z.D.A.; validation, Z.D.A. and J.S.M.; formal analysis, Z.D.A.; investigation, Z.D.A. and J.S.M.; resources, Z.D.A.; data curation, Z.D.A.; writing—original draft preparation, Z.D.A.; writing—review and editing, J.S.M. and M.M.A.; visualization, Z.D.A.; supervision J.S.M. and M.M.A.; funding acquisition, Z.D.A. All authors have read and agreed to the published version of the manuscript.

6.2. Data Availability Statement

The data presented in this study are available on request from the corresponding author.

6.3. Funding

The authors received no financial support for the research, authorship, and/or publication of this article.

6.4. Acknowledgements

The authors would like to thank the technical and faculty staff of the Civil Engineering Department at the University of Technology, Baghdad, Iraq, for their valuable support and scientific assistance.

6.5. Conflicts of Interest

The authors declare no conflict of interest.

7. References

[1] Wohl, E. E. (1998). Uncertainty in Flood Estimates Associated with Roughness Coefficient. Journal of Hydraulic Engineering, 124(2), 219–223. doi:10.1061/(asce)0733-9429(1998)124:2(219).

[2] Ballesteros, J. A., Bodoque, J. M., Díez-Herrero, A., Sanchez-Silva, M., & Stoffel, M. (2011). Calibration of floodplain roughness and estimation of flood discharge based on tree-ring evidence and hydraulic modelling. Journal of Hydrology, 403(1–2), 103–115. doi:10.1016/j.jhydrol.2011.03.045.

[3] Salmasi, F., Ayaseh, A., Dalir, A. H., & Arvanaghi, H. (2019). Flow pattern study in Beshar River and its two straight and meander reaches using CCHE2D model. Applied Water Science, 10(1), 19. doi:10.1007/s13201-019-1107-5.

[4] Whiting, P. J., & Dietrich, W. E. (1993). Experimental Studies of bed topography and flow patterns in large-amplitude meanders: 2. Mechanisms. Water Resources Research, 29(11), 3615-3622. doi:10.1029/93WR01756.

[5] Whiting, P. J., & Dietrich, W. E. (1993). Experimental constraints on bar migration through bends: Implications for meander wavelength selection. Water Resources Research, 29(4), 1091–1102. doi:10.1029/92WR02356.

[6] Blanckaert, K. (2009). Saturation of curvature-induced secondary flow, energy losses, and turbulence in sharp open-channel bends: Laboratory experiments, analysis, and modeling. Journal of Geophysical Research: Solid Earth, 114(3), 1-23. doi:10.1029/2008JF001137.

[7] Ülke, A., Beden, N., Demir, V., & Menek, N. (2017). Numerical modeling of Samsun Mert River floods. European Water, 57, 27-34.

[8] Hsieh, T. Y., & Yang, J. C. (2003). Investigation on the Suitability of Two-Dimensional Depth-Averaged Models for Bend-Flow Simulation. Journal of Hydraulic Engineering, 129(8), 597–612. doi:10.1061/(asce)0733-9429(2003)129:8(597).

[9] Darby, S. E., Alabyan, A. M., & Van de Wiel, M. J. (2002). Numerical simulation of bank erosion and channel migration in meandering rivers. Water Resources Research, 38(9), 21. doi:10.1029/2001wr000602.

[10] Brunner, G. W. (2016). HEC-RAS River Analysis System: Hydraulic Reference Manual Version 5.0. US Army Corps of Engineers-Hydrologic Engineering Center (HEC), Davis, United States.

[11] Elbashir, M. A. O. (2019). 2D hydraulic modelling of a braided river system using aerial imagery for water depth mapping: The Wairau River. Master Thesis, Institute of Hydrology and Meteorology, Wellington, New Zealand.

[12] Kayyun, T. S., & Dagher, D. H. (2018). 2D-Unsteady Flow within a Reach in Tigris River. International Journal of Scientific & Engineering Research, 9(5), 2246–2251.

[13] Alwan, I., Majeed, Z., & Abbas, A. (2021). Water Flow Simulation of Tigris River Between Samara and Baghdad Based on HEC-RAS Model. Engineering and Technology Journal, 39(12), 1882–1893. doi:10.30684/etj.v39i12.1804.

[14] Vedmani, R., Panda, R. K., & Pandey, V. K. (2020). Calibration and Validation of HEC-RAS Model for Minor Command in Coastal Region. International Journal of Current Microbiology and Applied Sciences, 9(2), 664–678. doi:10.20546/ijcmas.2020.902.082.

[15] Donald V. C. (2017). Application of Two -Dimensional Hydraulic Modeling in Riverine Systems Using. Master Thesis, University of Dayton, Ohio, United States.

[16] Ghimire, E. (2019). Evaluation of one-dimensional and two-dimensional HEC-RAS models for flood travel time prediction and damage assessment using HAZUS-MH a case study of Grand River. Master Thesis, Youngstown State University, Youngstown, United States.

[17] Balouchi, B., Ruther, N., Mirzaahmadi, A., & Schwarzwälder, K. (2022). Two-dimensional (2D) depth-averaged numerical modeling of a braided river morphodynamics upstream of a dam reservoir. 7th IAHR Europe Congress, 7-9 September, 2022, Athens, Greece.

[18] Parhi, P. K., Sankhua, R. N., & Roy, G. P. (2012). Calibration of Channel Roughness for Mahanadi River, (India) Using HEC-RAS Model. Journal of Water Resource and Protection, 04(10), 847–850. doi:10.4236/jwarp.2012.410098.

[19] Anderson, C. (2023). Using 2D HEC-RAS Modeling with Vertical Feature Extraction to Inform Ecological Design in the Lower Atchafalaya River Basin, Louisiana. Master Thesis, Colin Anderson, Louisiana State University and Agricultural and Mechanical College, Baton Rouge, United States.

[20] Kozak, J. P., Bennett, M. G., Piazza, B. P., & Remo, J. W. F. (2016). Towards dynamic flow regime management for floodplain restoration in the Atchafalaya River Basin, Louisiana. Environmental Science & Policy, 64, 118–128. doi:10.1016/j.envsci.2016.06.020.

[21] Khuzaiea, H. M. A. A., Awada, A. M., & Abbasa, M. F. (2018). A Hydraulic Model for Identification of Surface Friction Coefficient for Euphrates River within Al Muthanna Governorate, Iraq. Muthanna Journal of Engineering and Technology (MJET), 6(2), 160-168. doi:10.18081/mjet/2018-6/160-168.

[22] Hameed, L. K., & Ali, S. T. (2013). Estimating of Manning's roughness coefficient for Hilla River through calibration using HEC-RAS model. Jordan Journal of Civil Engineering, 7(1), 44-53.

[23] Hameed, L. K. (2014). Calibration of Manning' s Friction Factor for Rivers in Iraq Using Hydraulic Model (Al-Kufa River as Case study). International Journal of Innovative Science, Engineering & Technology, 1(10), 504–515.

[24] Serrano, J. S., Herrera, E. C., & Naito, K. (2024). Hydraulic Analysis of the Marikina River Floodplain During Typhoon Vamco using Numerical Modelling. Proceedings of IAHS, 386, 121–126. doi:10.5194/piahs-386-121-2024.

[25] Orozco, A. N. R., Bertrand, N., Pheulpin, L., Migaud, A., & Abily, M. (2023). Comparison Between HEC-RAS and TELEMAC-2D Hydrodynamic Models of the Loire River, Integrating Levee Breaches. New Modelling Paradigms for Water issues? 8-10 November, 2023, Chatou, France.

[26] Garg, C., & Ananda Babu, K. (2023). Extreme Flood Calibration and Simulation Using a 2D Hydrodynamic Model Under a Multipurpose Reservoir. Nature Environment and Pollution Technology, 22(2), 977–983. doi:10.46488/NEPT.2023.v22i02.042.

[27] Mawat, M. J., & Hamdan, A. N. A. (2023). Simulation of 2D depth averaged saint Venant model of Shatt Al Arab river south of Iraq. International Journal of Design and Nature and Ecodynamics, 18(3), 583–592. doi:10.18280/ijdne.180310.

[28] Mohamed, M. J., Karim, I. R., Fattah, M. Y., & Al-Ansari, N. (2023). Modelling Flood Wave Propagation as a Result of Dam Piping Failure Using 2D-HEC-RAS. Civil Engineering Journal (Iran), 9(10), 2503–2515. doi:10.28991/CEJ-2023-09-10-010.

[29] Al-Ansari, N., Adamo, N., Sissakian, V. K., Knutsson, S., & Laue, J. (2018). Water Resources of the Tigris River Catchment. Journal of Earth Sciences and Geotechnical Engineering, 8(3), 1792–9660.

[30] Kareem Abed, A. R., Hobi, M. H., & Jabbar Jihad, A. (2014). Numerical Modeling of Sediment Transport Upstream of Al-Ghammas Barrage. International Journal of Scientific & Engineering Research, 5(11), 469–477.

[31] Hobi, M. H. (2014). Analytical Study of Haditha Reservoir Sedimentation by CFD Model. Journal of Babylon University / Engineering Sciences, 22(2), 2014.

[32] Mahmood, M. S., Almurshedi, K. R., & Hashim, Z. N. (2017). Non-linear regression models for hydraulic geometry relationships in Al-Abbasia meandering reach in Euphrates river. Jordan Journal of Civil Engineering, 11(4), 549–556.

[33] Ministry of Water Resources (2023). General Authority for Dams and Reservoirs Dams, Directorate Najaf Branch, Najaf, Iraq.

[34] USGS (2023), Science for a Changing World. U.S. Department of Interior, Washington, United States Available online: https://earthexplorer.usgs.gov/ (accessed on January 2024).

[35] USACE. (2023). HEC-RAS 2D User's Manual, Version 6.3. U.S. Army Corps of Engineers, Washington, United States

[36] Chow, V.T. (1959) Open Channel Hydraulics. McGraw-Hill, New York, United States.

[37] Esri (2024). GIS Mapping Software, Location Intelligence & Spatial. Available online: https://www.esri.com/en-us/home (accessed on March 2023).

[38] Refsgaard, J. C., & Henriksen, H. J. (2004). Modelling guidelines—terminology and guiding principles. Advances in Water Resources, 27(1), 71–82. doi:10.1016/j.advwatres.2003.08.006.

[39] Kannan, N., Santhi, C., White, M. J., Mehan, S., Arnold, J. G., & Gassman, P. W. (2019). Some challenges in hydrologic model calibration for large-scale studies: A case study of SWAT model application to Mississippi-Atchafalaya River Basin. Hydrology 6(1), 17. doi:10.3390/hydrology6010015.

[40] Mustafa, A. S., Sulaiman, S. O., & Al_Alwani, K. M. (2017). Application of HEC-RAS model to predict sediment transport for Euphrates River from Haditha to Heet 2016. Al-Nahrain Journal for Engineering Sciences, 20(3), 570-577.

[41] Akay, H. Ü. S. E. Y. İ. N., Koçyiğit, B., & Yanmaz, A. M. (2016). a case study for determination of hydrological parameters in HEC-HMS in computing direct runoff. 12th International Congress on Advances in Civil Engineering (ACE) at Istanbul, 21-23 September, 2016, Istanbul, Turkey.